Cylindrical-confinement-induced phase behaviours of diblock copolymer melts*

Liu Mei-Jiao(刘美娇), Li Shi-Ben(李士本)†,
Zhang Lin-Xi(章林溪), and Wang Xiang-Hong(王向红)

Department of Physics, Wenzhou University, Wenzhou 325035*, China*

(Received 17 June 2009; revised manuscript received 27 July 2009)

The phase behaviours of diblock copolymers under cylindrical confinement are studied in two-dimensional space by using the self-consistent field theory. Several phase parameters are adjusted to investigate the cylindrical-confinement-induced phase behaviours of diblock copolymers. A series of lamella-cylinder mixture phases, such as the mixture of broken-lamellae and cylinders and the mixture of square-lamellae and cylinders, are observed by varying the phase parameters, in which the behaviours of these mixture phases are discussed in the corresponding phase diagrams. Furthermore, the free energies of these mixture phases are investigated to illustrate their evolution processes. Our results are compared with the available observations from the experiments and simulations respectively, and they are in good agreement and provide an insight into the phase behaviours under cylindrical confinement.

Keywords: cylindrical confinement, phase behaviour, diblock copolymer, self-consistent field theory

PACC: 8120S, 8200

1. Introduction

Geometric confinement naturally occurs in the self-assembly of block copolymers. The confined surface can break the bulk balance between the entropy of system and the interfacial energy, therein the blocks can be reorganized under confinement. Therefore, directly controlling the confinement conditions can generate novel microstructures that are not available in the bulk. This provides an important approach to the fabrication of microstructures, which have great potential applications in nanotechnology including the lithographic templates for nanoparticle synthesis, photonic crystals, and high-density information storage media.[1−6]

The self-assembled microphases of diblock copolymers have attracted great interest in the confinement in different integral dimensions in experiment,[7−9] theory[10−18] and simulation.[15,19−29] For example, the microphases of diblock copolymers have been extensively investigated for two-dimensional (2D) confinement, the cylindrical pore confinement.[15,26,30] For the lamella-forming diblock copolymers, the concentric lamella (CL) phases have been demonstrated by the transmission electron microscopy (TEM),[7−9] the Monte Carlo (MC) simulation,[15,24,26,27,31] and the self-consistent field theory (SCFT).[32] In these cases, the flat lamellae were frustrated into the lamellar structures with the cylindrical symmetry, known as the CL phases, meeting the requirement of cylindrical confinement. The multi-layer CL phase can be formed when the confinement degree is suitable, where their thicknesses can be predicted by the strong-stretching theory (SST),[15] and analysed by the MC and the SCFT methods.[15,26,32] More complex frustrated structures, such as helix and toroids, have been observed for the cylinder-forming diblock copolymers by means of the SCFT, the MC and the experimental methods.[7−9,12,13,23,26] In particular, the asymmetric diblock copolymers confined in the cylindrical nanopores with strong strengths of surface fields have been studied by using the MC method in the three-dimensional (3D) space.[23,26] In their studies, the volume fractions were selected to be $f_{\rm A} = 1/6$ and $f_{\rm A} = 1/4$ in the strong segregation regions, respectively, and confinement degrees were varied to investigate the phase behaviours. These studies revealed that the structural frustrations could be observed when the cylinder repeat period mismatches the pore diameter, also depending on the surface field strength.

However, the diblock copolymers adopted in those

*Project supported by the National Natural Science Foundation of China (Grant Nos. 20574052 and 20774066), the Program for New Century Excellent Talents in University, China (Grant No. NCET-05-0538) and the Natural Science Foundation of Zhejiang Province, China (Grant Nos. R404047, Y4090174, and Y405553).

†Corresponding author. E-mail: shibenli@wzu.edu.cn

© 2010 Chinese Physical Society and IOP Publishing Ltd

studies are usually limited to two or three fixed phase parameters. In the present work, the phase diagrams are arranged as the volume fraction and segregation degree, as well as the surface field strength and the confinement degree. We employ the SCFT calculation method to investigate the confinement-induced phase behaviours of diblock copolymers through their phase diagrams under the cylindrical confinement in 2D space, and mainly concern the novel phases observed in the phase diagrams and their evolvements in the pseudo-dynamic processes. The rest of the present paper is organized as follows. In Section 2, the SCFT method is briefly introduced, and the results are presented in Section 3, in which we discuss the phase behaviours with different phase parameters by comparing them with the available simulation results. Conclusions are drawn in Section 4 finally.

2. Calculation and method

We consider a system of AB diblock copolymers confined in a cylindrical pore of diameter D and volume V. The volume fractions of A and B blocks are f_{A} and f_{B}, respectively. We assume that A and B segments have equal statistical segment length a, and each copolymer has the same degree of polymerization N. The n linear AB diblock copolymers are regarded as the Gaussian chains with radius of gyration, R_{g}. In Edward's theory, a Gaussian chain is assumed to be related to a diffusion behaviour of a particle, which can be described by the propagator, $q(\boldsymbol{r}, s)$, the probability of any monomerappearing at $\boldsymbol{r}$ position. Here, $\boldsymbol{r}$ is the distance from the pore surface along the diameter direction. Because the two ends of polymer chain are different, so there is another diffusion form described as conjugated $q^*(\boldsymbol{r}, s)$. Here $q(\boldsymbol{r}, s)$ and $q^*(\boldsymbol{r}, s)$ should hold for the following modified diffusion equations,

$$\frac{\partial}{\partial s} q\left(\boldsymbol{r}, s\right) = \begin{cases} R_{\mathrm{g}}^2 \nabla^2 q\left(\boldsymbol{r}, s\right) - N\omega_{\mathrm{A}}\left(\boldsymbol{r}, s\right) q\left(\boldsymbol{r}, s\right), & 0 < s \leq f_{\mathrm{A}}, \\ R_{\mathrm{g}}^2 \nabla^2 q\left(\boldsymbol{r}, s\right) - N\omega_{\mathrm{B}}\left(\boldsymbol{r}, s\right) q\left(\boldsymbol{r}, s\right), & f_{\mathrm{A}} < s \leq 1, \end{cases} \tag{1}$$

and

$$\frac{\partial}{\partial s} q^*\left(\boldsymbol{r}, s\right) = \begin{cases} -R_{\mathrm{g}}^2 \nabla^2 q^*\left(\boldsymbol{r}, s\right) + N\omega_{\mathrm{A}}\left(\boldsymbol{r}, s\right) q^*\left(\boldsymbol{r}, s\right), & 0 < s \leq f_{\mathrm{A}}, \\ -R_{\mathrm{g}}^2 \nabla^2 q^*\left(\boldsymbol{r}, s\right) + N\omega_{\mathrm{B}}\left(\boldsymbol{r}, s\right) q^*\left(\boldsymbol{r}, s\right), & f_{\mathrm{A}} < s \leq 1. \end{cases} \tag{2}$$

Here s is the parameter that increases continuously from 0 to 1 along the chain. The mean field $\omega\left(\boldsymbol{r}, s\right)$ originates from the repulsion interaction between the A and B blocks. The initial conditions of Eqs. (1) and (2) are $q\left(\boldsymbol{r}, 0\right) = 1$ and $q^*\left(\boldsymbol{r}, 1\right) = 1$. Furthermore, the partition function of a single diblock copolymer can be expressed as

$$Q = \int \mathrm{d}\boldsymbol{r} q\left(\boldsymbol{r}, s\right) q^*(\boldsymbol{r}, s). \tag{3}$$

Within the mean-field approximation to the many-chain Edward's theory, the free energy per chain in the unit of $k_{\mathrm{B}}T$ is given as follows:[10,16,18,33]

$$\frac{F}{nk_{\mathrm{B}}T} = -\ln\left(\frac{Q}{V}\right) + \frac{1}{V}\int \mathrm{d}r \left[\chi_{\mathrm{AB}} N\phi_{\mathrm{A}}\phi_{\mathrm{B}} - \omega_{\mathrm{A}}\phi_{\mathrm{A}} - \omega_{\mathrm{B}}\phi_{\mathrm{B}} + U_{\mathrm{A}}\phi_{\mathrm{A}} + U_{\mathrm{B}}\phi_{\mathrm{B}} - P\left(\phi_0 - \phi_{\mathrm{A}} - \phi_{\mathrm{B}}\right)\right], \tag{4}$$

where the logarithmic term, $-\ln\left(Q/V\right)$, represents the entropy from the chain stretching; the integral term denotes the comprehensive effect from the repulsion interaction between A and B blocks, and the confinement fields from inner surface of the cylindrical pore; χ_{AB} is Flory–Huggins parameter that characterizes the repulsion between the A–B monomers; $\chi_{\mathrm{AB}}N$ denotes the degree of separation; U_{A} and U_{B} represent the short-range surface fields from the inner surface of the confinement acting on A and B monomers, respectively; P is a Lagrange multiplier as a pressure to ensure the incompressibility of the system.

Once the free energy of the system is given, we can obtain the equilibrium parameters by minimizing the free energy with respect to the monomer density and mean field. This minimization leads to the following

SCFT equations:

$$\omega_{\rm A}(\boldsymbol{r}) = \chi_{\rm AB}(\phi_{\rm B}(\boldsymbol{r}) - f_{\rm B}) + U_{\rm A}(\boldsymbol{r}) + P(\boldsymbol{r}), \quad (5)$$

$$\omega_{\rm B}(\boldsymbol{r}) = \chi_{\rm AB}(\phi_{\rm A}(\boldsymbol{r}) - f_{\rm A}) + U_{\rm B}(\boldsymbol{r}) + P(\boldsymbol{r}), \quad (6)$$

$$\phi_{\rm A}(\boldsymbol{r}) = \frac{V}{Q}\int_0^{f_{\rm A}} {\rm d}sq(\boldsymbol{r},s)\,q^*(\boldsymbol{r},s), \quad (7)$$

$$\phi_{\rm B}(\boldsymbol{r}) = \frac{V}{Q}\int_{f_{\rm A}}^1 {\rm d}sq(\boldsymbol{r},s)\,q^*(\boldsymbol{r},s). \quad (8)$$

These SCFT equations can be successfully solved by the combinatorial screening method based on the real-space implementation, which is originally proposed by Drolet and Fredrickson.[34,35] The real-space implementation is suitable for the exploration of the novel morphologies of copolymer without requiring the assumption of the system symmetry. In the real-space algorithm, there is assumed a pseudo-dynamic process to search the equilibrium phases in the given parameters of system. Namely, the initial mean fields $\omega_{\rm A}$ and $\omega_{\rm B}$ are input for Eqs. (1) and (2) to obtain $q(\boldsymbol{r},s)$ and $q^*(\boldsymbol{r},s)$ at the beginning, while Q, $\phi_{\rm A}(\boldsymbol{r})$ and $\phi_{\rm B}(\boldsymbol{r})$ can be calculated according to Eqs. (3), (7) and (8), and then $F/nk_{\rm B}T$ are obtained from Eq. (4). In the next iteration step, the new free energy per chain $F/nk_{\rm B}T$ can be acquired by updating mean fields and repeating the above steps. The iteration step $N_{\rm s}$ continues until the difference between the new free energy per chain and the old ones (that is, the convergence criterion $\Delta F/nk_{\rm B}T$) reaches zero. Here, we take criterion of $\Delta F/nk_{\rm B}T < 10^{-11}$ in the calculation process to obtain the final equilibrium state. Each minimization of the free energies is run several times by using different random initial mean fields $\omega_{\rm A}$ and $\omega_{\rm B}$ to ensure that the exact equilibrium morphology is obtained.

Those iteration processes are performed in a PC cluster with 18 nodes, which is similar to that in our previous work.[33] We take $0.2R_{\rm g}$ as the lattice size in all calculations, and divide the length of the chain contour into 200 monomers. In order to realize the fact that at the confinement surface the polymer densities should approach zero, the incompressibility condition is modified as $\phi_{\rm A}(\boldsymbol{r}) + \phi_{\rm B}(\boldsymbol{r}) = \phi_0(\boldsymbol{r})$, and $\phi_0(\boldsymbol{r}) = 1$ in the pore, while $\phi_0(\boldsymbol{r}) = 0.5$ for the lattice next to the confinement surfaces. The surface preference $U_{\rm A(B)}$ reflects the short-range surface-polymer interaction between the pore surface and A(B) block, which can be simplified as $U_{\rm A(B)}(r) = \eta_{\rm A(B)}\chi N$ for the lattice next to the confinement surface. Here, the coefficient $\eta_{\rm A(B)}$ represents the reduced strength of surface field. In the present work, all the calculations are performed in 2D space in order to explore novel structures in the large confinement sizes that are unable to be realized in 3D space because of the limitation of computer capability.

3. Results and discussion

3.1. Phases transition with volume fraction and segregation degree

We investigate the phase transition due to the variation of the volume fraction $f_{\rm A}$ and segregation degree $\chi_{\rm AB}N$ in this section. We fix other two phase parameters, the surface field strength to be $U_{\rm A} = U_{\rm B} = 0$ and the pore diameter to be $D = 20R_{\rm g}$, and then increase $f_{\rm A}$ from 0.15 to 0.45 in steps of 0.05 and $\chi_{\rm AB}N$ from 15 to 80. We plot the phase diagram arranged as the $f_{\rm A}$ and $\chi_{\rm AB}N$ in Fig. 1 where the typical phases are also indicated. Furthermore, we record the free energy of an especial phase in the pseudo-dynamic process to explore its evolvement in Fig. 2, and discuss the several characteristics of CL phases in Fig. 3.

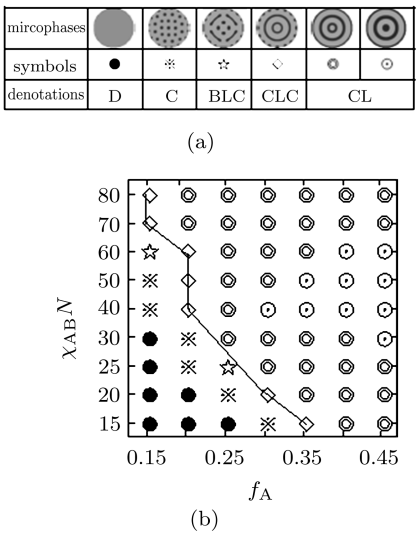


Fig. 1. Phase behaviours induced by the volume fraction $f_{\rm A}$ and segregation degree $\chi_{\rm AB}N$. (a) The morphologies; (b) the phase diagram. The diblock copolymers are confined in the cylindrical pores with the diameter $D = 20R_{\rm g}$ and the neutral surfaces. Here, the black and the gray colours represent A-block and B-block respectively (Note that the same forms in the following figures).

Several typical phases with their symbols and denotations are shown in Fig. 1(a). As we expected, the disordered (D), cylinder (C) and lamella phases appear in the cylindrical pores. However, the classical spherical phase is not observed due to the 2D structure, and the cylinders are not hexagonally but cylin-

drically arranged in the pores because of the cylindrical confinement. Due to the same reason, the lamella phase in bulk changes into the CL phase, which has been extensively observed in the previous studies as mentioned before. It is interesting that we have observed two mixture phases, i.e. the mixture of broken lamellae and cylinders (BLC) and the mixture of concentric lamellae and cylinders (CLC). The similar CLC phase has been observed in the pore with radius $R = 8.5R_{\rm g}$ where the CL phase appears near the pore surface because the surface is preferable to one block.[32] Here, the cylinder components of CLC phase distribute near the pore surfaces in a non-hexagonal manner, while the CL structures occur in the inner zone of pore. The BLC phase is somewhat similar to the CLC phase, which has the cylinder component near the surface. But, the outer layer of CL structure is broken and the inner layer changes into the cylinders.

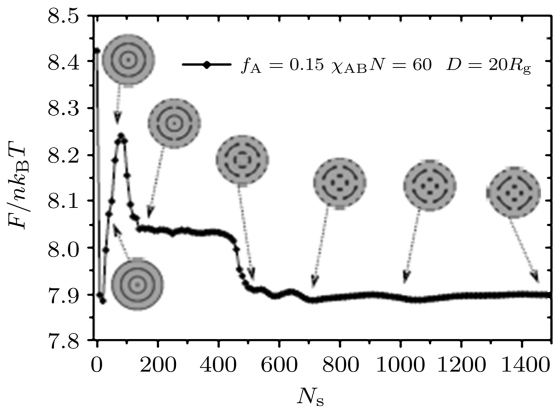


Fig. 2. Free energy per chain $F/nk_{\rm B}T$ as a function of iteration step $N_{\rm s}$. The morphologies are inserted at the corresponding positions to illustrate the evolvement process of BLC phase. The BLC phase parameters are selected to be $f_{\rm A} = 0.15$, $\chi_{\rm AB}N = 60$ and $D = 20R_{\rm g}$.

Then, we discuss the phase behaviours in the confined phase diagram as shown in Fig. 1(b). When $f_{\rm A} \geq 0.35$, the diblock copolymers exhibit the CL phases for any segregation degree except for $\chi_{\rm AB}N = 15$. For a fixed $f_{\rm A}$, a different block domain appears in the centre of CL structure as $\chi_{\rm AB}N$ increases. The previous work has reported on a similar phenomenon observed by varying the confinement degree where the pore surface was preferable to the block.[26] The present observation indicates that the segregation degree can also result in the variation of block domain in the pore centre. For $f_{\rm A} < 0.35$, the diblock copolymers undergo the relatively complicated phase transitions. For example, the diblock copolymers begin with D phase for the weak segregation at $f_{\rm A} = 0.20$, and evolve into the C phase and CLC phase, finally to the CL phase with the value of $\chi_{\rm AB}N$ increasing. This fact indicates that the confined diblock copolymers tend to the lamella phase for the fixed $f_{\rm A}$ as the segregation degree increases. It is reasonable to deduce that the diblock copolymers have a tendency to be of lamella phase for the most $f_{\rm A}$ in the strong segregation limit. This deduction is also in agreement with the bulk phase diagram.[36,37] However, the diblock copolymers have a more complicated behaviour

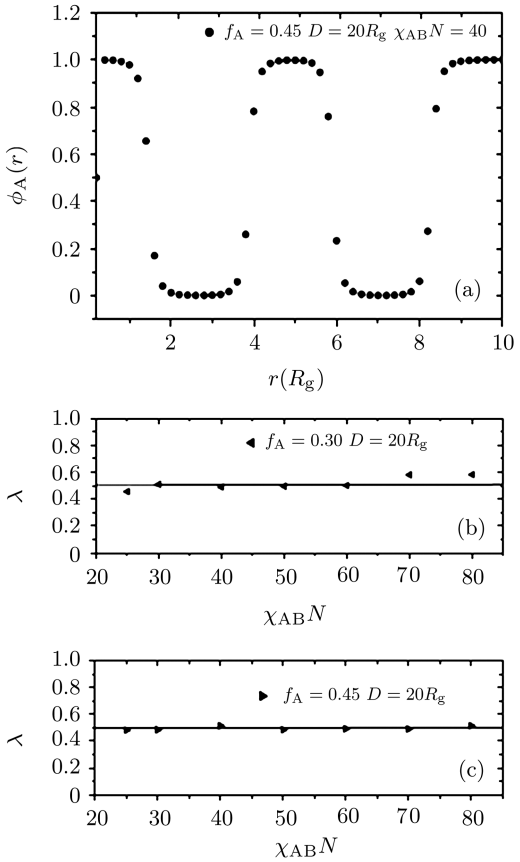


Fig. 3. Illustration of CL phase. (a) The monomer density $\phi_{\rm A}(r)$ as a function of r, where r is the distance from the pore surface along the diameter direction. Here, $f_{\rm A} = 0.45$, $\chi_{\rm AB}N = 40$, and $D = 20R_{\rm g}$. (b) The ratio λ as a function of segregation degree for $f_{\rm A} = 0.30$. (c) The ratio λ as a function of segregation degree for $f_{\rm A} = 0.45$. The λ denotes the ratio of the thickness of the outmost layer to the average one of other A-rich layers inside.

than those in the limit of strong segregation. For instance, the phase is transformed from the C phase to the CLC and CL phases at $\chi_{\rm AB}N = 40$ as $f_{\rm A}$ increases from 0.15 to 0.25. When $f_{\rm A}$ increases, there is enough connection of A segment to form the CL structure, which has also been observed by Feng *et al.*

in the study of hydrophobic–hydrophilic copolymers confined in hydrophobic nano-cylindrical tubes.[38]

Although this phase diagram is much rougher in the f_A and $\chi_{AB}N$ than the bulk phase diagram,[36,37] it still has several similar characteristics. First, the lamella phase occupies the most of phase space in the bulk diagram, while there is the CL phase in the confined diagram. Meanwhile, the C and D phases occupy relatively small phase space in the confined one. Secondly, these confined phases are located at the similar positions to the bulk ones. However, there are more complex phases appearing in the phase boundary than in the phase boundary in the bulk diagram, as shown in Fig. 1(b). This is due to the fact that the diblock copolymers located near the confined phase boundary are easy to deform into the complex phases.[13] Since the phase diagram is obtained in the pore with neural surface, our phase diagram has the symmetry about the f_A, which is different from the previous diagram with a slightasymmetry about the f_A due to the surface preferential to one block.[32]

Then, we discuss the evolvement process of BLC phase, an especial structure on the boundary of the phase diagram. We select the parameters to be $f_A = 0.15$ and $\chi_{AB}N = 60$, and obtain the BLC phase. Taking advantage of recording the free energy in the pseudo-dynamic process, the F/nk_BT–N_s curve is obtained and used to discuss the evolvement of cylinder phase of cylinder-forming diblock copolymers confined in thin film.[17] Here, according to Eq. (4) we have plotted the free energy per chain F/nk_BT as a function of iteration step N_s in Fig. 2, in which the corresponding morphologies are inserted at the suitable positions for the convenience of illustrating the evolvement. Obviously, there are three stages in the evolvement process of BLC phase. The first stage is to make a random adjustment at $N_s \approx 0$–100. In this stage, the initial mean fields ω_A and ω_B are randomly input at the beginning of the evolvement, and then the free energy fluctuates abruptly. We should note that the lowest free energy at $N_s \approx 30$ originates from the random adjustment process, which does not represent the equilibrium state in this stage although the diblock copolymer exhibits the CL phase with three concentric layers of A blocks in this stage. Another reason is that these states do not satisfy the convergence criterion of $\Delta F/nk_BT < 10^{-11}$. Actually, this random process is similar to that observed in the cylinder-forming diblock copolymers in thin film where the lowest values of free energies have also been observed.[17] The second stage is a process of layer breaking at $N_s = 100$–520, in which the layers are broken one by one. The outmost layer begins to break into the cylinders distributed near the pore surface at $N_s = 100$. Then, the second outmost layer is disconnected at $N_s = 140$, while the interior layer is separated into four parts at $N_s = 520$. The third stage is to make an adjustment of the BLC phase where the broken layers are adjusted to the final structure. Although all the layers are separated at $N_s = 520$, they are not a stable phase at this iteration step because of $\Delta F/nk_BT > 10^{-5}$. The free energy is slightly fluctuated in this stage until $\Delta F/nk_BT < 10^{-11}$ at $N_s = 10000$ (not marked in the figure). Under this convergence criterion, we obtain the BLC phase with a minimal free energy, i.e. $F_m/nk_BT = 7.891130$. From the free energy curve, we can conclude that the free energy decreases abruptly at the iteration step of layer breaking. It is an evidence that the free energies are 8.24064, 8.03967 and 7.90862 at $N_s = 100$, 140, and 520, respectively, when three layers are broken from the pore surface to its centre one by one.

In fact, the BLC phase evolvement process can be explained based on the symmetry breaking. Since the CL structure has a high cylindrical symmetry, the conformation of diblock copolymer is adjusted to the CL structure at the first stage due to the cylindrical symmetry originating from the cylindrical confinement. However, the diblock copolymer is in the form of cylinder that will self-assemble into the hexagonally arranged cylinders with non-cylindrical symmetry in bulk. In order to meet this requirement, the concentric layers begin to break into the cylinders one by one. In other words, the symmetry breaking results in the phenomenon that the free energy decreases abruptly in the iteration step of layer breaking while the cylinders and broken-lamella components are layered and arranged in the pore. The symmetry breaking exists extensively in the confined self-assembly process, which can be used to reasonably explain the other types of confinement-induced phases.[18,32,33,39]

As shown in Fig. 1(b), the CL phase is the most popular phase in the confined phase diagram. The same phenomenon is also shown in real-space self-consistent mean-field theory simulations of Li *et al.*, where the CL structures were labeled as L_2 and L_3.[32] The CL structures have been observed in the Monte Carlo simulations of He *et al.*,[27] in the dynamical density functional simulations of Sevink *et al.*[40] and also in the experiments of Russell *et al.*[41] Here, we

discuss this confinement induced phase by investigating the monomer density and layer thickness in Fig. 3. First, we select the phase parameters to be $f_{\rm A}$=0.45, $\chi_{\rm AB}N = 40$, and $D = 20R_{\rm g}$, and plot $\phi_{\rm A}(r)$ as a function of r (in units of $R_{\rm g}$) in Fig. 3(a). The sharp variation of the monomer density reflects that A and B blocks are separate completely in the cylindrical pore because of the strong separation, indicating the rigid characteristic.[42] For the CL phases, the A- or B-rich layer appears alternatively in the pore centre for the different values of $f_{\rm A}$ and $\chi_{\rm AB}N$, while minority A blocks always occur near the neutral surfaces. The fact exhibits that the surface is preferable to the minority block in despite of the neutral surface, and the outmost layer is thinner than the other minority-block layers inside. This phenomenon is known as the hard-surface effect,[14] which has been observed in the MC and dissipative particle dynamics (DPD) simulations.[26,31,43] Here, we observe this effect in the CL phase with the detailed data as shown in Figs. 3(b) and 3(c), separately, in which the λ denotes the ratio of the thickness of the outmost layer to the average of the other A-rich layers. The result of $\lambda \approx 0.5$ quantitatively confirms the argument that the hard-surface effect takes place as $\chi_{\rm AB}N$ varies.

3.2. Phase transition induced by surface field and confinement degree

The phase transition not only can be induced by $f_{\rm A}$ and $\chi_{\rm AB}N$, but also can be affected by the surface field $\eta_{\rm A(B)}$ and the pore diameter D (which represents the confinement degree). The previous studies have concentrated on the effects of surface field and confinement degree on the diblock copolymers confined in the cylindrical pores.[23,25,26,44,45] In this section, we select the parameter to be $f_{\rm A} = 0.2$ and $\chi_{\rm AB}N = 60$ (that is, the BLC phase in Fig. 1(b)) to investigate the effects of surface field preferable to the minority blocks in Fig. 4 and preferable to the majority blocks in Fig. 5. In both cases, the pore diameter D varies from $8R_{\rm g}$ to $32R_{\rm g}$ and the reduced strength of surface field $\eta_{\rm A(B)}$ increases from 0 to 1. Then, we will discuss the evolvement process of an especial phase in Fig. 6.

Figure 4 is a phase diagram arranged as $\eta_{\rm A}$ versus D. Here, we reveal several general characteristics from this phase diagram. The first characteristic is that the cylinder component distributes cylindrically near the pore surfaces for the weak value of $\eta_{\rm A}$. However, when the value of $\eta_{\rm A}$ increases up to a certain degree, the lamella structure occurs for all values of D. These cylindrical distributions are consistent with the experimental results for the cylinder-form diblock copolymers confined in the pore.[7,8] The second characteristic is that the A- or B-rich domain appears alternatively in the pore centre for all given values of $\eta_{\rm A}$ as the value of D increases, which has been observed in experiment and accords with the previous results.[7,25] As a whole, the middle layers of CL phase are not influenced by the surface field $\eta_{\rm A}$, and the phase behaviour seems relatively simple. This is mainly due to the surfaces preferable to the minority blocks, which reduces the effect of surface field $\eta_{\rm A}$.

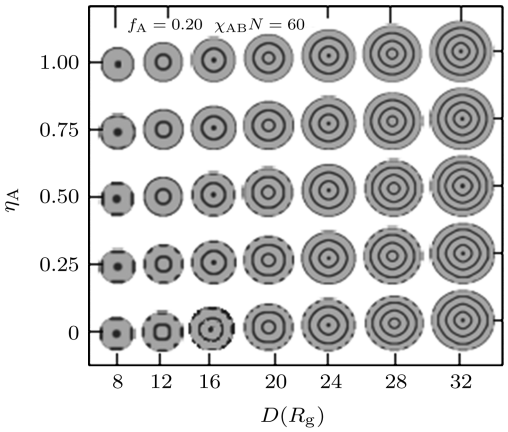


Fig. 4. Phase diagram arranged as surface field $\eta_{\rm A}$ versus confinement degree D. The diblock copolymer parameters are selected to be $f_{\rm A} = 0.20$ and $\chi_{\rm AB}N = 60$.

However, this is not the case for the surfaces preferable to the majority blocks because of asymmetric blocks for the copolymers as shown in Fig. 5. We observe the different phase behaviours for the different confinement degrees in this phase diagram. For example, for the severe confinement of $D = 12R_{\rm g}$, when there is no field, i.e. $\eta_{\rm B} = 0$, we observe the morphology with two layers where the outermost layer is in the form of cylindrically arranged cylinder and the cylindrical lamella occurs in the inner layer in the A-block domain as shown in Fig. 5. When the value of $\eta_{\rm B}$ increases from 0 to 0.5, the inner layer maintains unchanged while the cylindrical form of outermost layer is adjusted from irregular to regular. Continuously the increasing of $\eta_{\rm B}$ value leads to the deformation of both the inner and the outermost layers. Namely, the broken square lamella structure appears in the outermost layer while the cylinders are square arranged in the inner layer at $\eta_{\rm B} = 0.75$. For the strong surface field of $\eta_{\rm B} = 1.00$, the morphology evolves into the CL structure due to the strong cylindrical sym-

metry of the surface field. For the moderate confinement degree of $D = 20R_g$, the weak surface field cannot affect the morphology and the diblock copolymers maintain the CLC phase when the value of η_B increases from 0 to 0.25. However, it is interesting that a complicated morphology, a mixture of square-lamellae and cylinders (SLC), can be observed at $\eta_B = 0.50$. Then, the diblock copolymers transit into the BLC phase at $\eta_B = 0.75$ and the mixture phase of concentric-lamellae and cylinders at $\eta_B = 1.00$. The SLC phase has an obvious square symmetry because the cylinder and the square-lamella components distribute squarely in 2D space. We think that the SLC phase is due to the competition between confinement degree and surface field. Since the diblock copolymers are confined in the cylindrical pore, they exhibit somewhat bulk characteristic, i.e. the flat symmetry, when the space is suitable (determined by the confinement degree). On the other hand, the diblock copolymers exhibit cylindrical symmetry which can be strengthened by the surface field. In order to confirm this argument, we investigate the phase behaviours in a weak confinement degree. For $D = 32R_g$, a similar SLC phase also appears at $\eta_B = 0.50$. However, this SLC phase is slightly different from those observed in a moderate confinement degree where there is multilayer CL phase appearing in the inner zone, and the innermost layer is not the squarely symmetrical for the weak confinement degree, which supports our argument.

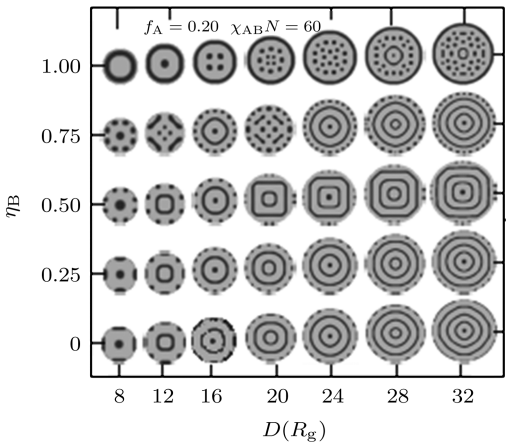


Fig. 5. Phase diagram arranged as surface field η_B versus confinement degree D. The diblock copolymer parameters are selected to be $f_A = 0.20$ and $\chi_{AB}N = 60$.

For a given value of η_B, several general characteristics can be obtained by varying the confinement degree. For the weak surface preference of $\eta_B = 0.25$, the diblock copolymers have similar morphologies to those for neutral surfaces due to the weak interactions between surfaces and blocks. When the surface field η_B increases up to a value of 0.50, i.e., $\eta_B = 0.50$, we observe the SLC phases for various D. This result indicates that the SLC phase is sensitive to surface field, and the cylindrical symmetry is easy to break at a moderate strength of surface field. For $\eta_B = 1.00$, the diblock copolymers assemble into the morphology composed of a layer of cylindrical lamella and several layers of cylindrically distributing cylinders, owing to the strong cylindrical symmetry from the strong surface field. This phase is similar to those LC phases observed in the previous work.[32] The previous MC studies also confirmed the cylindrical symmetry of morphologies for strong surface field in 3D space where the surface field parameter was selected to be $\alpha = 1.00$.[23,26]

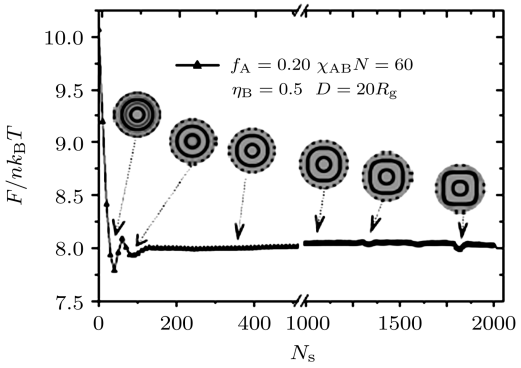


Fig. 6. Free energy per chain F/nk_BT as a function of iteration step N_s. The morphologies are inserted at the corresponding positions to illustrate the evolvement process of SLC phase. The SLC phase parameters are selected to be $f_A = 0.20$, $\chi_{AB}N = 60$, $\eta_B = 0.50$, and $D = 20R_g$.

The SLC phase is an especial morphology that is observed for the first time. We perform the further investigation on this phase and plot the free energy per chain F/nk_BT as a function of iteration step N_s in Fig. 6. Here the phase parameters are selected to be $\eta_B = 0.5$, $D = 20R_g$, $f_A = 0.20$ and $\chi_{AB}N = 60$, and the diblock copolymer exhibits an standard SLC phase according to the phase diagram. As shown in Fig. 6, there are three stages to form the SLC morphology, similar to the formation of BLC phase. First, the evolution process begins with inputting the random ω_A and ω_B, and the F/nk_BT decreases sharply because the phase begins to separate. When the iteration step N_s is increased to 40, there is a CL structure with incomplete separation between A and B blocks. This is not a stable phase because it does not satisfy the free energy criterion. Then, F/nk_BT begins to increase and then decreases when the diblock copolymer

begins to form CLC morphology within $N_s = 40$–80. Similar to the case observed in Fig. 2, the free energy with the lowest value also originates from the random adjustment process, which is not a stable or metastable state. In the second stage, the diblock copolymers spend a long iteration step to undergo the CLC phase until $N_s = 1000$. Actually, this CLC phase is a metastable phase in this evolvement process. We have observed the metastable phases of diblock copolymers under other confinements by using a similar method.[13,33] The last stage is an adjustment one. In this stage, a part of A-blocks on the outmost layer turns into ones inside layers because the surface is preferable to the B blocks so that few cylinders remain in the outmost layer. At the same time, the outer layers of CL structure are adjusted to be square lamella structure while the inner layer of CL structure remains unchanged. The inner layer with the smaller diameter is hard to pull into square lamella, due to the rigid characteristic for the diblock copolymers.[42] Therefore, the diblock copolymer exhibits the SLC phase in the equilibrium state.

4. Conclusions

In this paper, we preformed the SCFT calculation to study the confinement-induced phase behaviours for the diblock copolymer melts in 2D space. The effects of phase parameters including f_A, $\chi_{AB}N$, $U_{A(B)}$ and D on phase behaviour are investigated in detail. A great variety of novel phases of confined diblock copolymers are observed where the corresponding phase behaviours are also discussed in phase evolvement.

First, f_A and $\chi_{AB}N$ can induce complex phase behaviours of diblock copolymers under cylindrical confinement. We find that the cylindrical-confinement can induce the CL structure in most phase zones for the diblock copolymers, especially in the strong segregation zones. A series of complicated phases, such as the CLC and BLC phases, is observed near the phase boundary in the phase diagram, indicating that it is easy to deform the phase of diblock copolymers in this zone. Secondly, we investigated the phase behaviours induced by $U_{A(B)}$ and D for the cylinder-forming diblock copolymer. For the surface preferable to the majority blocks, the different confinement degrees result in distinct phase behaviours. We find that the moderate confinement degree and surface field lead to the SLC phase, which can be understood by the competition between these two phase parameters.

For the especial and interesting phases, the BLC and SLC phases, we discussed their evolvement by recording their free energies in the iteration processes, respectively. The fact indicates that the BLC and the SLC have similar evolvement processes. They both undergo three stages from random adjustment to the lamella structure break, and to the slight adjustment of the final equilibrium phases. Our results are compared with the available observations from the experiments and simulations, which are in good agreements.

References

[1] Park C, Yoon J and Thomas E L 2003 *Polymer* **44** 6725

[2] Lazzari M and Lopez-Quintela M A 2003 *Advanced Materials* **15** 1583

[3] Fu C F, Wei Y Y, Duan Z Y, Wang W X and Gong Y B 2009 *Chin. Phys.* B **18** 2749

[4] Zhang Q Y 2009 *Chin. Phys.* B **18** 658

[5] Li X, Zhai F F, Liu Y, Cao M S, Wang F C and Zhang X X 2007 *Chin. Phys.* **16** 2769

[6] Li J, Zhang K W, Meng L J, Liu W L and Zhong J X 2008 *Acta Phys. Sin.* **57** 382 (in Chinese)

[7] Xiang H Q, Shin K, Kim T, Moon S I, McCarthy T J and Russell T P 2004 *Macromolecules* **37** 5660

[8] Xiang H Q, Shin K, Kim T, Moon S I, McCarthy T J and Russell T P 2005 *Macromolecules* **38** 1055

[9] Sun Y, Steinhart M, Zschech D, Adhikari R, Michler G H and Gosele U 2005 *Macromol. Rapid Commun.* **26** 369

[10] Matsen M W 1997 *J. Chem. Phys.* **106** 7781

[11] Huinink H P, Brokken-Zijp J C M, Dijk M A V and Sevink G J A 2000 *J. Chem. Phys.* **112** 2452

[12] Li W H and Wickham R A 2006 *Macromolecules* **39** 8492

[13] Chen P, Liang H J and Shi A C 2007 *Macromolecules* **40** 7329

[14] Meng D and Wang Q 2007 *J. Chem. Phys.* **126** 234902

[15] Wang Q 2007 *J. Chem. Phys.* **126** 024903

[16] Chen P, Liang H J and Shi A C 2008 *Macromolecules* **41** 8938

[17] Heckmann M and Drossel B 2008 *Macromolecules* **41** 7679

[18] Yang Y Z, Qiu F, Zhang H D and Yang Y L 2006 *Polymer* **47** 2205

[19] Ren C L, Chen K and Ma Y Q 2005 *J. Chem. Phys.* **122** 154904

[20] Li M and Zhu Y J 2008 *Acta Phys. Sin.* **57** 7555 (in Chinese)

[21] Wang Q, Yan Q, Nealey P F and Pablo J J D 2000 *J. Chem. Phys.* **112** 450

[22] Wang Q, Nealey P F and Pablo J J D 2001 *Macromolecules* **34** 3458

[23] Yu B, Sun P C, Chen T H, Jin Q H, Ding D T, Li B H and Shi A C 2006 *Phys. Rev. Lett.* **96** 138306
[24] Chen P, He X H and Liang H J 2006 *J. Chem. Phys.* **124** 104906
[25] Yu B, Li B H, Jin Q H, Ding D T and Shi A C 2007 *Macromolecules* **40** 9133
[26] Yu B, Sun P C, Chen T H, Jin Q H, Ding D T, Li B H and Shi A C 2007 *J. Chem. Phys.* **127** 114906
[27] He X H, Song M, Liang H J and Pan C Y 2001 *J. Chem. Phys.* **114** 10510
[28] Ren C L and Ma Y Q 2005 *J. Am. Chem. Soc.* **128** 2733
[29] Ren C L and Ma Y Q 2005 *Phys. Rev.* E **72** 051804
[30] Sevinka G J A and Zvelindovsky A V 2008 *J. Chem. Phys.* **128** 084901
[31] Feng J and Ruckenstein E 2006 *Macromolecules* **39** 4899
[32] Li W H, Wickham R A and Garbary R A 2006 *Macromolecules* **39** 806
[33] Li S B, Chen P, Wang X H, Zhang L X and Liang H J 2009 *J. Chem. Phys.* **130** 014902
[34] Drolet F and Fredrickson G H 1999 *Phys. Rev. Lett.* **83** 4317
[35] Fredrickson G H, Ganesan V and Dorlet F 2002 *Macromolecules* **35** 16
[36] Matsen M W and Schick M 1994 *Phys. Rev. Lett.* **72** 2660
[37] Matsen M W and Bates F S 1996 *Macromolecules* **29** 1091
[38] Feng J and Ruckenstein E 2008 *J. Chem. Phys.* **128** 074903
[39] Yu B, Sun P C, Chen T H, Jin Q H, Ding D T, Li B H and Shi A C 2007 *J. Chem. Phys.* **126** 204903
[40] Sevink G J A, Zvelindovsky A V, Fraaije J G E M and Huinink H P 2001 *J. Chem. Phys.* **115** 8226
[41] Shin K, Xiang H Q, Moon S I, Kim T, McCarthy T J and Russell T P 2004 *Science* **306** 76
[42] Wang Q, Nealey P F and De Pablo J J 2002 *Macromolecules* **35** 9563
[43] Feng J, Liu H L and Hu Y 2006 *Macromol. Theory Simul.* **15** 674
[44] Wang Z, Li B H, Jin Q H, Ding D T and Shi A C 2008 *Macromol. Theory Simul.* **17** 86
[45] Yu B, Jin Q H, Ding D T, Li B H and Shi A C 2008 *Macromolecules* **41** 4042